Chemosphere 313 (2023) 137373

Contents lists available at ScienceDirect

Chemosphere

journal homepage: www.elsevier.com/locate/chemosphere

Laser-based techniques: Novel tools for the identification and characterization of aged microplastics with developed biofilm

Pavel Pořízka [a,b], Lukas Brunnbauer [c], Michaela Porkert [c], Ula Rozman [d], Gregor Marolt [d], Daniel Holub [b], Martin Kizovský [e], Markéta Benešová [e], Ota Samek [e], Andreas Limbeck [c], Jozef Kaiser [a,b], Gabriela Kalčíková [d,*]

[a] Central European Institute of Technology, Brno University of Technology, Purkyňova 656/123, 61200, Brno, Czech Republic
[b] Faculty of Mechanical Engineering, Brno University of Technology, Technická 2896/2, 61669, Brno, Czech Republic
[c] TU Wien, Institute of Chemical Technologies and Analytics, Getreidemarkt 9/164-I²AC, 1060, Vienna, Austria
[d] Faculty of Chemistry and Chemical Technology, University of Ljubljana, Večna Pot 113, 1000, Ljubljana, Slovenia
[e] Institute of Scientific Instruments, Czech Academy of Sciences, Královopolská 147, 612 64, Brno, Czech Republic

HIGHLIGHTS

- Microplastics were aged in freshwater and wastewater.
- Advanced laser-based techniques were tested for the detection of aged microplastics.
- Raman spectroscopy detected and classified aged microplastics.
- LIBS detected microplastics and biotic elements in the developed biofilm.
- LA-ICP-MS detected metals in microplastics and in the developed biofilm.

GRAPHICAL ABSTRACT

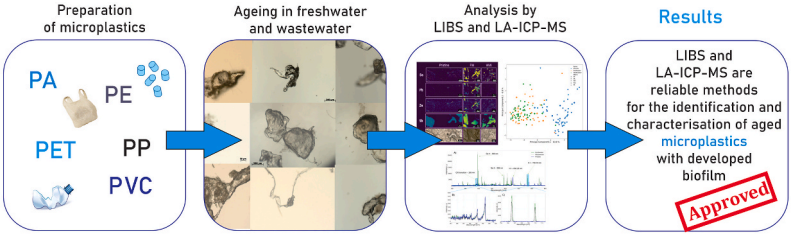

ARTICLE INFO

Keywords:
Ageing
Biofilm
Detection
Microplastics
Spectroscopic methods

ABSTRACT

Microplastics found in the environment are often covered with a biofilm, which makes their analysis difficult. Therefore, the biofilm is usually removed before analysis, which may affect the microplastic particles or lead to their loss during the procedure. In this work, we used laser-based analytical techniques and evaluated their performance in detecting, characterizing, and classifying pristine and aged microplastics with a developed biofilm. Five types of microplastics from different polymers were selected (polyamide, polyethylene, polyethylene terephthalate, polypropylene, and polyvinyl chloride) and aged under controlled conditions in freshwater and wastewater. The development of biofilm and the changes in the properties of the microplastic were evaluated. The pristine and aged microplastics were characterized by standard methods (e.g., optical and scanning electron microscopy, and Raman spectroscopy), and then laser-induced breakdown spectroscopy (LIBS) and laser ablation inductively coupled plasma mass spectrometry (LA-ICP-MS) were used. The results show that LIBS could identify different types of plastics regardless of the ageing and major biotic elements of the biofilm layer. LA-ICP-MS showed a high sensitivity to metals, which can be used as markers for various plastics. In addition, LA-ICP-MS can be employed in studies to monitor the adsorption and desorption (leaching) of metals

* Corresponding author.
E-mail address: gabriela.kalcikova@fkkt.uni-lj.si (G. Kalčíková).

https://doi.org/10.1016/j.chemosphere.2022.137373
Received 19 August 2022; Received in revised form 21 November 2022; Accepted 22 November 2022
Available online 23 November 2022

during the ageing of microplastics. The use of these laser-based analytical techniques was found to be beneficial in the study of environmentally relevant microplastics.

1. Introduction

Plastic pollution is an omnipresent problem, and small pieces of plastic, called microplastics (MPs), are currently a focus of scientists and society (SAPEA, 2019). The diversity of MP sources leads to high variability in MP types; they are made of different polymers and they vary in size and shape (Rozman and Kalčíková, 2022). In addition, their properties may be significantly altered by the surrounding environment, because in wastewater and freshwater, MPs are rapidly colonized by various microorganisms that form a biofilm. The developed biofilm changes the properties of MPs (e.g., size, density), and thus, their fate in the environment (Kalčíková et al., 2020; He et al., 2022). Moreover, biofilm also camouflages the MPs, which limits their reliable detection and analysis.

Traditionally, the detection of MPs in environmental samples is carried out by microscopy, with their identification based on their physical appearance. However, MPs can be confused with natural fibres or other particles (Song et al., 2015). Therefore, visual identification is often coupled with spectroscopic methods, such as Fourier-transform infrared spectroscopy (FTIR) or Raman spectroscopy, to confirm the composition of the investigated particles (Mariano et al., 2021). Prior to the spectroscopic analysis, MPs are pre-treated to remove adsorbed organic and inorganic matter or developed biofilm by acidic, alkaline, or enzymatic digestion (Hermsen et al., 2018). However, these methods lack the ability to localise MPs directly in the environmental matrix (e.g., adhered to tissues, present in organs) and suffer from the potential destruction and loss of particles. Therefore, there is an urgent need for new analytical methods and approaches that allow for the direct detection of aged MPs in the environmental matrices and biota.

In this context, the use of advanced laser-based analytical techniques, namely laser-induced breakdown spectroscopy (LIBS) and laser ablation inductively coupled plasma mass spectrometry (LA-ICP-MS), could be a promising approach for the direct analysis of MPs. LIBS can detect different types of plastic due to its unique spectral response to specific polymers (Anzano et al., 2014; Liu et al., 2019; Gajarska et al., 2021), and it showed a good performance in polymer classification based namely on variations in CN and C_2 band intensities (Chamradová et al., 2021). LA-ICP-MS, on the other hand, can detect marker metals in polymers (Stehrer et al., 2010; Bonta et al., 2016) and indicate polymer alterations (Brunnbauer et al., 2020). To date, LIBS and LA-ICP-MS have been used to a limited extent for the direct detection of MPs, and both have been used mainly for monitoring trace metals adsorbed on MPs (Chen et al., 2020; El Hadri et al., 2020, respectively). Sommer et al. (2021) successfully used LIBS to identify MPs extracted from sediment samples. However, prior to the analysis, the samples were pre-treated by Fenton oxidation to remove organic and inorganic matter, so the performance of the method for direct analysis was not tested. Similarly, Michel et al. (2020) compared different spectroscopy techniques (attenuated total reflectance – Fourier-transform infrared spectroscopy (ATR-FTIR), X-ray fluorescence (XRF), near-infrared (NIR) reflectance spectroscopy, and LIBS) for the detection of MPs sampled in the marine environment, but again, the MPs were pre-treated and the organic and inorganic matter was removed before the analysis. To the best of our knowledge, a thorough study of pristine and aged MPs has never been conducted using either individual laser-based techniques or their combination.

In this work, laser-based techniques were used as alternative techniques to characterize pristine and aged (in freshwater and wastewater) MPs. First, Raman spectroscopy was used to test its ability to classify MPs regardless of ageing and to demonstrate its established position in polymer analysis. Second, laser-based techniques (LIBS and LA-ICP-MS) were used to characterize MPs based on their elemental fingerprints. LIBS was used for the direct classification of MPs based on their major element signature, while LA-ICP-MS targeted the marker metals within the cores of the MPs.

2. Materials and methods

This study was divided into three main parts: (i) different types of MPs were aged in freshwater and wastewater to obtain particles highly covered with biofilm, (ii) standard microscopy and Raman spectroscopy characterizations of MPs were provided as conventional methods, (iii) and finally, we studied LIBS and LA-ICP-MS for a complementary characterization and identification of pristine and aged MPs.

2.1. Microplastics characterization

Five different MPs, made of polyamide (PA), polyethylene (PE), polyethylene terephthalate (PET), polypropylene (PP), and polyvinyl chloride (PVC), were prepared from larger pieces of plastic by grinding in a centrifugal mill (ZM 200, Retsch, Germany). The PA, PE, and PP were pellets about 5 cm in size, while the PET and PVC were larger pieces of a plastic bottle and plastic pipes, respectively. During grinding, the blades were cooled with dry ice, so the mill was fed alternating pieces of plastic and dry ice. The mill had 12 blades, and the grinding speed was 15,000 rpm. The mesh size of the screens used to separate the smaller particles (already ground) from the larger particles was 500 μm when grinding PA, PE, and PP and 250 μm when grinding PVC and PET. Raman spectroscopy was used to confirm the material composition (Section 2.4).

Surface analysis of the MPs was performed using an optical microscope (Imager.Z2m, Zeiss, Germany) and field emission scanning electron microscopy (FE-SEM, Ultra plus, Zeiss, Germany) under different magnifications.

The particle size of the pristine MPs was measured using a laser diffraction analyser (S3500 Bluewave, Microtrac, Germany). Approximately 0.5 g of MPs was placed in the dry unit, and the measurement was repeated three times. The results were expressed as the number particle size distribution.

The density of the MPs was determined according to ISO 1183-1 (2019). A dried pycnometer was weighed before and after the addition of approximately 50 mg of MPs. Then, ethanol (96%) was added to the pycnometer, and it was weighed again. This was repeated for ethanol only. The density was calculated as follows:

$$\rho_{MPs} = \frac{m_2 - m_1}{m_2 - m_1 - m_3 + m_4} \cdot \rho_{ET}$$

where ρ_{MPs} (g/cm^3) is the density of the MPs, m_1 (g) is the mass of the empty pycnometer, m_2 (g) is the mass of the pycnometer and MPs, m_3 (g) is the mass of the pycnometer with MPs and ethanol, m_4 (g) is the mass of the pycnometer and ethanol, and ρ_{ET} (g/cm^3) is the density of the ethanol. The measurement was repeated three times.

2.2. Ageing of microplastics

MPs were incubated in freshwater and wastewater to simulate their ageing and the development of a natural biofilm. Each type of MP was aged separately. Freshwater was collected from the Glinščica stream (Slovenia), while wastewater came from a municipal wastewater treatment plant and was collected with an automatic water sampler as a 24 h combined sample after mechanical treatment. The ageing procedure largely followed the method described by Jemec Kokalj et al. (2019).

Briefly, the ageing of MPs was performed in 500 mL Erlenmeyer flasks; two flasks were prepared per MP and water type. The concentration of MPs was 5 g/L to ensure sufficient material for further analysis. All flasks were shaken throughout the ageing experiment (four weeks). Flasks containing MPs aged in freshwater were incubated at room temperature (22 ± 2 °C) under daylight fluorescent lamps (1200–1500 lx) with 16/8 h photoperiod (light/dark) at 125 rpm. Flasks containing MPs aged in wastewater were also incubated at room temperature (22 ± 2 °C) and 125 rpm, but they were kept in the dark to simulate the ageing of MPs in wastewater in the sewer system. At the beginning of each week, the MPs were filtered from all flasks (4–12 μm pores, Whatman®), and the recovered MPs were added to a new fresh sample of freshwater and wastewater. After a four-week ageing period, all MPs were filtered and stored at −18 ± 2 °C for further analysis.

Aged MPs were analysed for density again (as described above), and the biofilm mass and chlorophyll content were determined. To determine the mass of the biofilm, MPs with a developed biofilm (three replicates) were dried to constant weight at room temperature (22 ± 2 °C), and then the biofilm on the MPs was digested by Fenton oxidation (Prata et al., 2019). In Fenton oxidation, iron ions (Fe^{2+}) catalyse the decomposition of hydrogen peroxide (H_2O_2) into hydroxyl radicals (•OH) (Shokri and Fard, 2022), which oxidise the biofilm. After Fenton oxidation, the MPs were reweighed, and the results were expressed as mg of biofilm per g of MPs. The content of chlorophyll *a* in the biofilm developed on the MPs was determined using a method described by Kalčíková et al. (2016) with some modifications. Approximately 50 mg of MPs with a developed biofilm (three replicates) was homogenized with 1.8 mL of cold 95% (*v/v*) ethanol (−18 ± 2 °C) in a mortar with pestle. The absorbance of the supernatant was measured at 664 nm and 648 nm (Synergy LX, Biotek, USA). The concentration of chlorophyll *a* was calculated according to Lichtenthaler (1987) and expressed as mg of chlorophyll *a* per g of biofilm. The same procedure was applied to MPs (without biofilm) and the absorbance values were similar to the blank sample (ethanol only), indicating that the MPs themselves did not interfere with the measurement.

2.3. Reference analysis of elemental composition

Various metals used as additives in plastics (i.e. compounds of Ti, Zn, Co, Pb, Sb, Al, Ba, Cd (Hahladakis et al., 2018)) were determined. Pristine and aged MPs were digested using microwave-assisted digestion. Approximately 30 mg of dried sample was placed in a Teflon vessel with 4.5 mL HNO_3 (65%) and 0.5 mL 30% H_2O_2. The mixture was heated to 220 °C for 20 min in a microwave oven (Ethos Up, Milestone, Italy), and the temperature was maintained at 220 °C for the next 15 min. Fully digested samples were quantitatively transferred into 50-mL flasks and diluted with 1% HNO_3. The metal concentrations (measured as isotopes: ^{47}Ti, ^{66}Zn, ^{59}Co, ^{208}Pb, ^{121}Sb, ^{27}Al, ^{137}Ba, ^{111}Cd) were determined by ICP-MS (Agilent 7900ce, Agilent Technologies, USA) using an internal standard. The results were calculated as μg of metal per mg of MPs.

2.4. Raman spectroscopy

All Raman measurements were conducted on a Raman spectrometer (inVia, Renishaw, UK). The experiments were performed with a laser wavelength of 785 nm at 100% power (140 mW). There is an option to use a 532 nm laser as well, but the Raman spectra were covered with overwhelming fluorescence at this laser wavelength. The spectrometer was set to a 1200 cm^{-1} central Raman shift to detect all the important polymer peaks. An objective with 20× magnification (Leica, Germany) was used to focus the laser beam on the sample. Five different locations of each sample were measured by 10× accumulated 1 s expositions.

The resulting spectra were processed using a custom script in Python. The spectra were background-corrected by polynomial fitting (order 5) and rescaled to [0,1] (i.e., the minimal value was set to 0 and the maximal to 1). The mean of all 5 acquired spectra was used to compare the results. In the end, to highlight the differences among the various sample types, the spectra were compared in a raw (untreated) state.

The processed Raman spectra were then submitted to principal component analysis (PCA). The PCA algorithm provides dimensionality reduction of the data set, which is useful in the spectroscopic field as a tool to overlook the acquired data set. The PCA algorithm used in this work is part of the sklearn library (Pedregosa et al., 2011) in the Python programming language. In order to get the best possible PCA results, the data were mean-centred and scaled to the whole spectral range. The data set used for PCA in this section included all measured spectra.

2.5. Laser-induced breakdown spectroscopy (LIBS)

For all LIBS measurements, the FireFly LIBS system (Lightigo, Czech Republic) was employed. In the experiment, the system was equipped with a 532 nm laser that operated at 5 mJ. The pulse duration was 7 ns, and the spot size was approximately 150 μm, resulting in a fluence of approx. 120 GW/cm^2. The plasma emission was collected by an optical system and transported by optical fibre to a broad-range echelle-type spectrometer (resolution λ/Δλ 6000) with a range of 200–900 nm and equipped with an EMCCD camera, which was set to a gate delay of 500 μs and a gate width of 50 μs The interaction area was purged by air during the experiment, which was found to be beneficial for the laser ablation of polymers in our previous work (Chamradová et al., 2021).

Prior to the LIBS analysis, the MPs were fixed onto epoxy resin; note that the experimental settings were based on previous experience with the ablation of the bulk plastic matrix. In this methodology, the MPs were located individually on the epoxy surface and ablated in a single-pulse regime. Each type of MP was measured on 10 distinct spots when two pulses per spot were used to diminish the influence of possible contamination. The collected data were then processed by a custom Python script and averaged to obtain the characteristic spectra of each MP type. The data treatment included outlier filtering using a normal distribution of total spectrum emissivity. The outlying 25% spectra per sample were omitted based on the total emissivity distribution.

The data set was handled similarly to the Raman spectroscopy data set (section 2.4.) and mean-centred and scaled to the whole spectral range. No additional filtering of the spectra or spectral ranges was carried out before the PCA analysis. The PCA was used according to the good LIBS practices described in previous works (Pořízka et al., 2018; Chamradová et al., 2021).

2.6. Laser ablation inductively coupled plasma mass spectrometry (LA-ICP-MS)

To investigate the possibility of distinguishing different MPs based on different inorganic additives present, a mixture of freshwater-aged PP, PET, and PVC particles was mounted in epoxy resin (Struers, Denmark). Individual samples of pristine and aged particles of all 5 polymer types were mounted in epoxy resin as well in order to investigate the lateral distribution of elements measured in the digested MPs (Section 2.3.) after freshwater/wastewater ageing. Cross-sections of these embedded samples were prepared by manual sanding using abrasive paper down to a grain size of 5 μm, and then LA-ICP-MS imaging experiments were carried out.

LA-ICP-MS analysis was carried out using an imageGEO193 laser ablation system (ESL, USA) operating at a wavelength of 193 nm and equipped with a TwoVol3 ablation chamber. The LA system was coupled to an iCAP Qc ICP-MS system (ThermoFisher Scientific, Germany) using Tygon® tubing with an inner diameter of 1.6 mm. Samples were ablated under a constant stream of helium (0.8 L/min). Argon was used as a make-up gas (0.8 L/min) and mixed with the sample aerosol using a dual concentric injector (DCI) (ESL, USA) right before the ICP. LA-ICP-MS data evaluation was carried out using Iolite 4.5.7.1. Additional measurement parameters are provided in Table S1.

Table 1
Mass of biofilm (mg/g of MPs), chlorophyll *a* content (mg/g of biofilm) and density (g/cm^3) of MPs. All parameters are expressed as mean ± SD (n = 3).

MPs	Mass of biofilm mg/g of MPs		Chlorophyll *a* mg/g of biofilm		Density (g/cm^3)		
	Freshwater	Wastewater	Freshwater	Wastewater	Pristine	Freshwater	Wastewater
PE	311 ± 60	357 ± 94	0.0770 ± 0.0084	0.0177 ± 0.0059	0.96 ± 0.02	1.04 ± 0.02	0.98 ± 0.00
PP	206 ± 16	168 ± 5	0.0635 ± 0.0178	0.0120 ± 0.0011	0.93 ± 0.04	1.18 ± 0.06	1.08 ± 0.13
PA	223 ± 29	219 ± 93	0.1848 ± 0.0341	0.0101 ± 0.0027	1.23 ± 0.03	1.13 ± 0.03	1.04 ± 0.01
PET	245 ± 23	197 ± 28	0.1085 ± 0.0062	0.0108 ± 0.0036	1.31 ± 0.01	1.18 ± 0.01	1.44 ± 0.06
PVC	194 ± 55	180 ± 77	0.0575 ± 0.0091	0.0139 ± 0.0005	1.12 ± 0.11	1.15 ± 0.02	1.19 ± 0.13

3. Results and discussion

3.1. Ageing and conventional characterization of microplastics

All MPs used in this study were in the form of white powder. SEM imaging showed all MPs had irregular shapes and low porosity (Fig. S1), typical of pristine MPs (Rozman et al., 2021). The PE MPs had a structurally more complex surface morphology in comparison to the other MPs (Fig. S1A). The polymer type of each pristine MP was confirmed by Raman spectroscopy (Section 3.2., Figs. S3–S7). The mean particle sizes (mean ± SD, n = 3) of the PE, PP, PA, PET, and PVC were 116.3 ± 68.0 μm, 357.0 ± 46.7 μm, 455.0 ± 49.1 μm, 23.1 ± 7.2 μm, and 157.4 ± 127.7 μm, respectively, which are the size ranges of MPs commonly found in freshwaters (Kameda et al., 2021; Lu et al., 2021). The mean particle size of the PET MPs was much smaller than that of the other MPs, and several very small MPs were also shown in the SEM images (Fig. S1D).

After ageing in freshwater and wastewater, the development of a biofilm on all MPs was confirmed (Table 1, Fig. S2). The MPs aged in wastewater formed heteroaggregates with present microorganisms (Fig. S2, e.g., PET FW, PE WW). The amount of developed biofilm was the highest on PE, while on the other MPs, it was comparable regardless of the MP polymer. This is in agreement with other studies where the morphology of the particles (i.e., surface roughness) played an important role in the biofilm development rather than the polymer composition or size of MPs (Parrish and Fahrenfeld, 2019; Miao et al., 2020). Microorganisms prefer to create a biofilm on various MPs (in comparison to natural substrates), as they tend to metabolize the polymer as a carbon source (Miao et al., 2020).

In the present study, the biofilms that developed on the MPs aged in freshwater contained significantly more photosynthetic microorganisms (expressed as chlorophyll *a* content) compared to the biofilms developed on the MPs aged in wastewater. The results are comparable for the PE, PP, and PET, while the chlorophyll *a* content was the lowest in the biofilm developed on the PVC (Table 1). PVC has been previously shown to reduce the chlorophyll *a* content in algal cells (Wang et al., 2020) and to affect other aquatic organisms, especially after ageing (Xia et al., 2022). The increased ecotoxicological risk can be attributed to the leaching of additives, such as phthalates (Henkel et al., 2019) and metals (Meng et al., 2021). The highest chlorophyll *a* content was measured in biofilms that developed on PA. Similarly, Venable and Podbielski (2019) suggested PA (nylon) as a good substrate material for algal growth.

The presence of a biofilm may alter the overall density of MPs, affecting their distribution in water, and thus, significantly influencing their fate in the aquatic environment (Li et al., 2018; Jalón-Rojas et al., 2022). In the case of PE, PP, and PVC, where the density of the pristine particles was below 1.2 g/cm^3, ageing in freshwater and wastewater increased the particle density (Table 1). Similarly, Lagarde et al. (2016) and Jalón-Rojas et al. (2022) reported an increase in the density of PP particles after incubation with the freshwater alga *C. reinhardtii* and in seawater, respectively. On the other hand, the pristine PA and PET had densities of 1.23 and 1.31 g/cm^3, respectively, and ageing in freshwater resulted in a decrease in the density, whereas the incubation in wastewater resulted in a decrease in the density of the PA, and the density of the PET increased. This could be explained by the variability in the mass

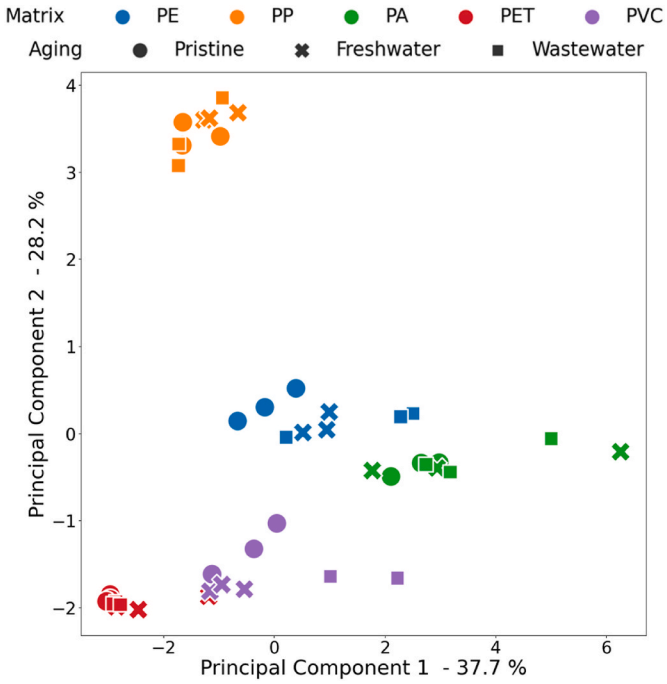

Fig. 1. Principal component analysis of all Raman spectra. The shapes of the data points depicts the pristine and aged MPs (in freshwater or wastewater); the colour shows the polymer type of MPs (PE, PP, PA, PET, PVC). (For interpretation of the references to colour in this figure legend, the reader is referred to the Web version of this article.)

of the biofilm (Table 1) as well as its composition, which is specific to each polymer (Tu et al., 2021). The density of biofilm ranges from 1.1 to 1.5 g/cm^3 (Long et al., 2015; Lagarde et al., 2016), and thus, the biofilm that develops on MPs can lead to an increase (in the case of low-density polymers) or a decrease (in the case of high-density polymers) in the density of aged MPs. The determined densities of the pristine MPs were consistent with the results of previous studies (Li et al., 2018; Shamskhany et al., 2021).

3.2. Characterization of aged microplastics by Raman spectroscopy

Although Raman spectroscopy is commonly used to characterize MPs sampled from the environment, the MPs are usually pre-treated to remove adsorbed organic and inorganic matter or developed biofilm (Xu et al., 2019). In this study, we characterized the pristine and aged MPs directly without any pre-treatment. All polymer types showed similar results with an increased fluorescent background in the case of MPs aged in freshwater and wastewater (Figs. S3–S7). The figures show a comparison of the spectra acquired from the same MP type that underwent different ageing methods, and all major peaks were identified and are highlighted at their referenced locations in all figures (Menchaca et al., 2003). The only difference among the spectra was the level of fluorescence, which is apparent in the raw spectra (Figs. S3–S7). In general, the

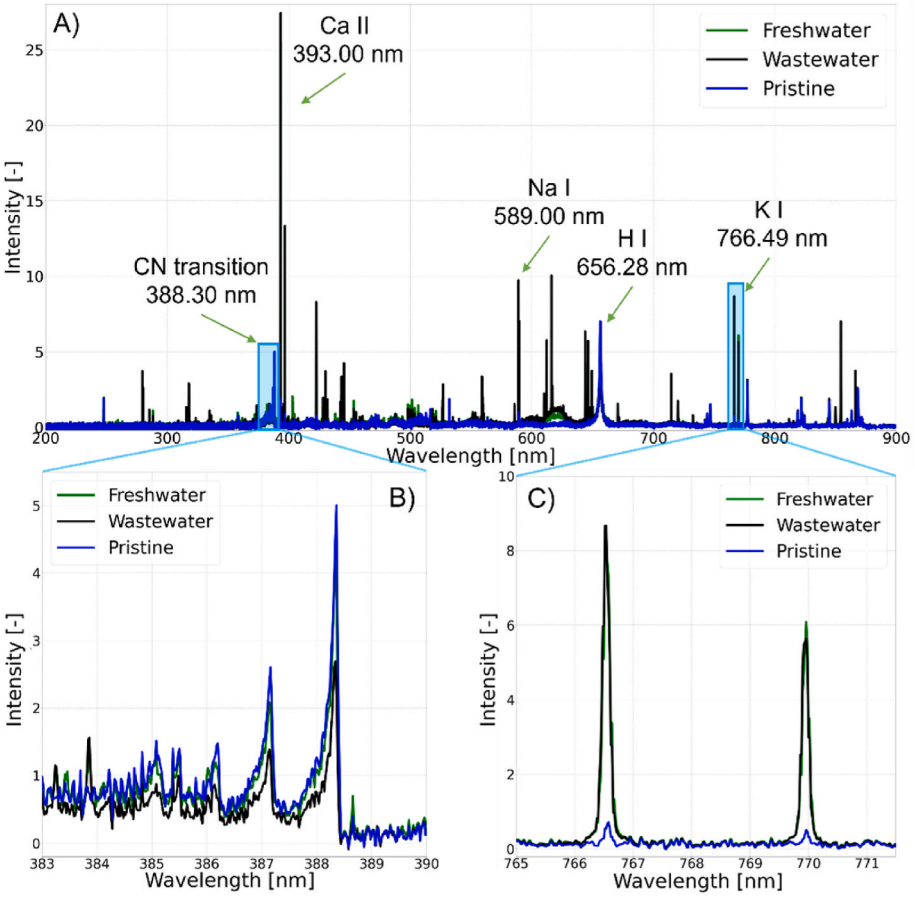

Fig. 2. (A) Comparison of spectra of pristine and aged PE (in freshwater and wastewater); (B) detail of CN transition area; (C) Detail of K I 766.49 nm and 769.89 nm area.

highest fluorescence occurred in the case of MPs aged in freshwater, most likely due to the presence of algae in the biofilm and the resulting increased content of chlorophyll *a* (Table 1), which naturally emits fluorescence (Strasser and Govindjee, 1992).

The ability of Raman spectroscopy to distinguish among all polymer types used in this study is highlighted in the results from PCA (Fig. 1). The background-corrected data set was used for PCA. After a standard data pre-treatment (scaling and mean-centring), the PC score plot was generated. We show the PC1 and PC2 score plots – this accounts for 66% of the variance within the data (Fig. S8). From this 2D PC score plot (Fig. 1), it is evident that the ageing process was not relevant for the classification of the plastic samples based on the Raman spectra. The spectra from the same polymer groups clustered together regardless of the ageing process. The most secluded data cluster was found for the PP.

3.3. Characterization of microplastics by laser-based techniques

3.3.1. Laser-induced breakdown spectroscopy (LIBS)

Although LIBS has been used previously to identify polymer types of plastic items (Junjuri et al., 2019; Chamradová et al., 2021), to the best of our knowledge, none of the published work has used LIBS to directly identify aged MPs without pre-treatment, and the only evidence for the applicability of this technique in MP research comes from Sommer et al. (2021) and Michel et al. (2020). However, in both studies, the biofilm and organic and inorganic matter were removed prior to analysis. In our work, the aged samples were processed directly without removing the biofilm, and the results show that even then, MPs can be detected.

The data collected by the LIBS were averaged and depicted to see the most prominent spectral lines. A comparison of the CN transition area of all pristine MPs is given in Fig. S9. Fig. 2 shows the results for PE as an example; the data for the other MPs (PA, PET, PP, and PVC) are given in the Supplementary Materials (Figs. S10–S13). A comparison of the pristine and aged MPs spectra showed that other biogenic elements were present in the aged MPs, e.g., Na, Ca, and K. On the contrary, the intensities of the H, C, and CN transition signals connected to the polymer structure were decreased in the aged MPs.

In our previous study, we classified bulk polymers based on their characteristic LIBS spectra obtained after laser ablation in various atmospheres (Chamradová et al., 2021). The CN band area around 388 nm had the biggest effect on the classification of polymers. Only two polymer types used in this study have been previously used. However, the results for these two polymers (PA and PP) correspond well to our former findings, and the CN band of the PA polymer type had a significantly lower intensity compared to PP. The CN band intensities split the polymer types into two groups: PP + PE + PET and PVC + PA. In our former work, the CN and C_2 transitions were used to classify different polymer types. The already known tendencies for the CN transition were obvious in the MP spectra here as well. These tendencies show that a higher C ratio in the monomer (as in the PET) and an increased simplicity of the monomer molecule (as in the PE and PP) resulted in a higher intensity of the CN transition. The lower success of the polymer type classification may be due to several factors, e.g., a lower number of spectra and non-uniform flatness of the ablated sample area.

To show the ability of LIBS to classify different MP types, we used PCA (Fig. 3) comprising reduced spectra by selecting wavelengths containing important information about the sample. The selected wavelengths were focused on the following area: the area of the CN transition and the Ca II peaks between 385 and 400 nm, the Na II 589 nm peak area, the H I 656.28 nm area, and the K I 766.49 nm peak area. These four areas should contain necessary information about the differences

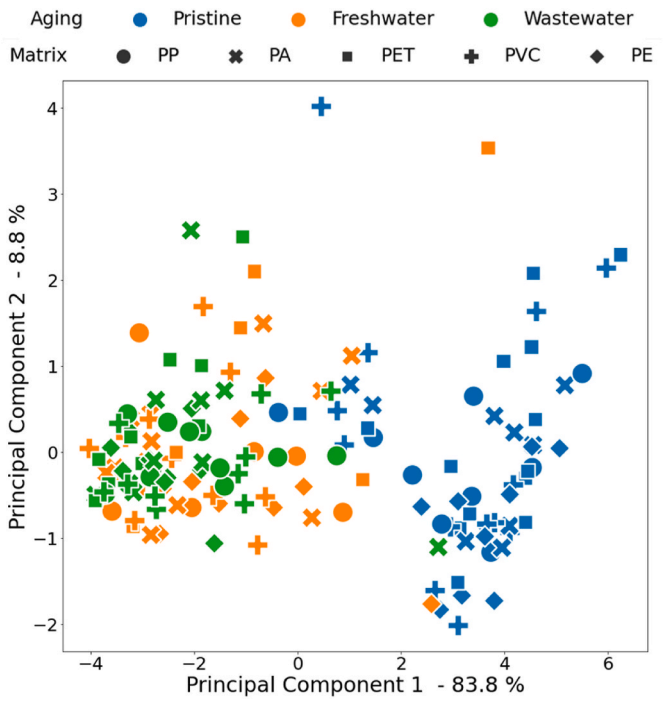

Fig. 3. Principal component score plot of filtered LIBS data. Shapes of data points depict the polymer types of MPs (PE, PP, PA, PET, PVC), whereas colours show the pristine and aged MPs (in freshwater or wastewater). (For interpretation of the references to colour in this figure legend, the reader is referred to the Web version of this article.)

between MPs. We used a data set with the selected wavelengths for PCA analysis. The data were also normalized, and the outliers were filtered. In this case, the first two PCs constituted 92.6% of the variance within the data. In this score plot, we were able to distinguish between the pristine MPs and aged MPs in the freshwater and wastewater. This was due to the increases in the Ca II, Na II, and K I peaks in the spectra of the aged MPs (see PCA loadings plot for truncated LIBS data (Fig. S14)). The classification of the aged MPs is problematic due to the high similarities of the polymer spectra.

3.3.2. *Laser ablation inductively coupled plasma mass spectrometry (LA-ICP-MS)*

3.3.2.1. Identification of MPs based on imaging of inorganic additives. Elements typically present as additives in polymers were used as markers to distinguish different polymer types. Digestion and liquid ICP-MS measurements (Table S2) revealed that significant amounts of Al were present in the PP ($Al(OH)_3$, which is typically used as a flame retardant (Marturano et al., 2017)). Zn was present in the PVC (ZnO is typically used as a biocidal additive (Vikhareva et al., 2021)), and Sb was present in the PET (Sb_2O_3 is typically used as a catalyst in PET manufacturing (Welle and Franz, 2011)). Mapping these elements in the MPs mounted in epoxy resin not only allowed for identifying the different polymer types present but also gives insight into the shapes of the individual MPs (Fig. 4). Looking only at the microscope picture of the mounted MPs, the identification of the three present polymer types (PP, PVC, PET) would not be possible. Comparing the distributions of the Al, Zn, and Sb obtained from the LA-ICP-MS imaging with a microscope picture revealed their identity. This example demonstrates the potential of LA-ICP-MS analysis for the localization and identification of MPs within solid samples.

It should be noted that in environmental samples containing more than three polymers, polymer types that have the same inorganic additives may occur. Thus, detecting one marker element is not specific to a particular polymer, which makes the distinction between different polymer types more challenging. Using a multielement approach of mapping the inorganic fingerprint of each polymer type combined with more advanced chemometric data evaluation may circumvent this problem.

3.3.2.2. Investigation of aged microplastics. Various elements (Al, Ba, Cd, Co, Pb, Sb, Ti, and Zn) were selected for LA-ICP-MS imaging experiments based on previously carried out digestion and liquid ICP-MS analysis of the MPs under investigation (Table S2). Mapping the cross-section of MPs aged in freshwater and wastewater and comparing the elemental distribution with pristine particles reveals whether MPs take up inorganic constituents or release inorganic additives into the environment. Moreover, these measurements also provide information about the local variations in the uptake of trace elements, particularly if there is an accumulation at specific parts of the MPs (e.g., near-surface regions) or if the uptake or release is homogeneous. Additionally, the accumulation of elements in the biofilm surrounding the particles can be investigated.

The elemental maps obtained for the individual PE and PET for a

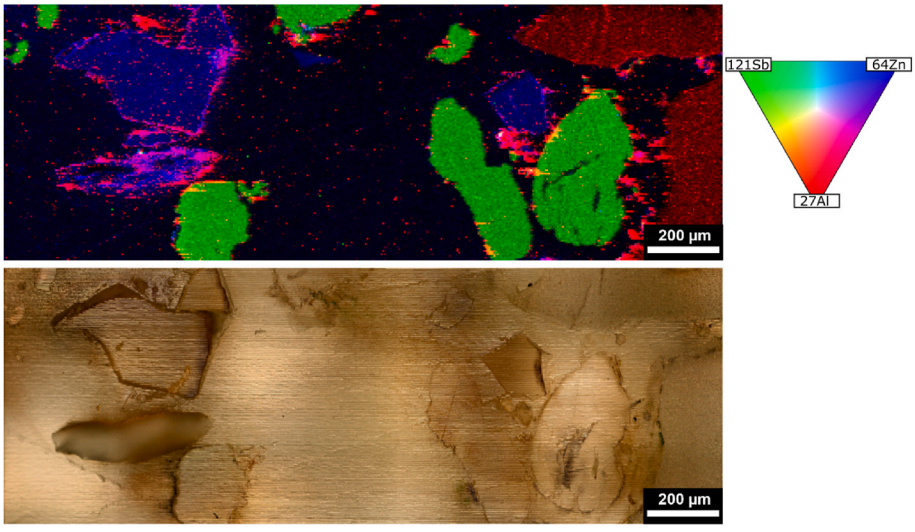

Fig. 4. Lateral distribution of marker elements obtained by LA-ICP-MS analysis revealed the distribution and shapes of the PP (Al), PVC (Zn), and PET (Sb) aged in freshwater.

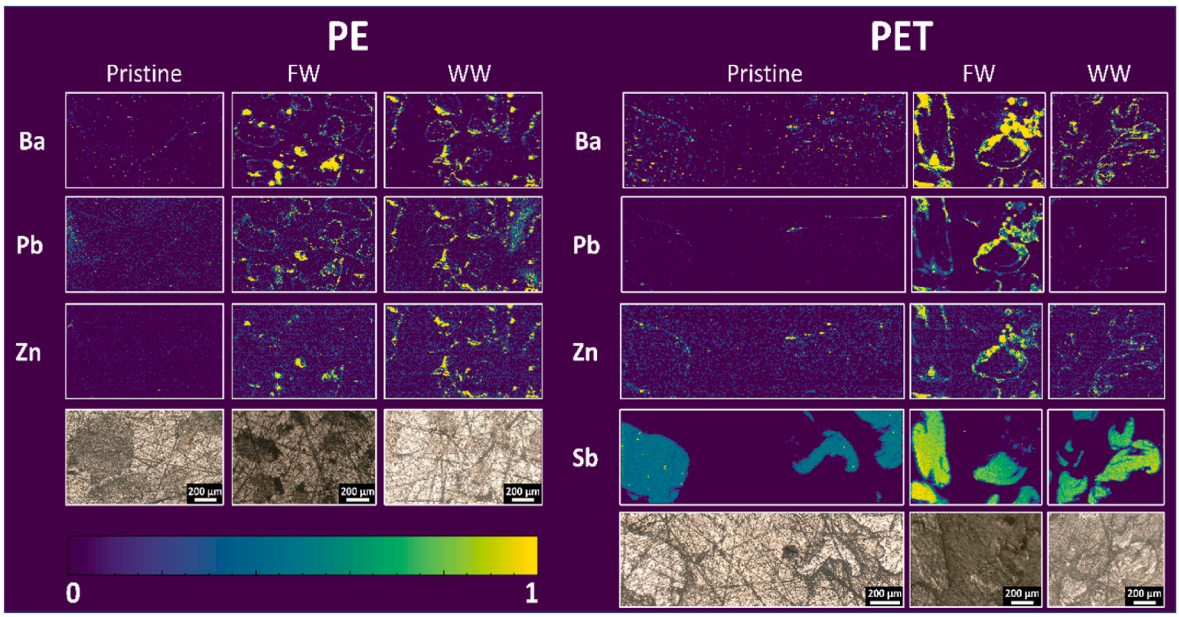

Fig. 5. LA-ICP-MS imaging of cross-sections of pristine and aged PE and PET MPs in freshwater (FW), and wastewater (WW), revealing the lateral distribution of Ba, Pb, Zn, and Sb.

selection of elements are shown in Fig. 5. The respective data for the other investigated polymer types and all analysed elements can be found in the Supplementary Materials (Figs. S15–19). The colour scale is the same for each element and each polymer type enabling a qualitative comparison between the pristine and aged MPs but not among the different polymer types.

The comparison of the elemental map of the pristine and aged PE in freshwater and wastewater (Fig. 5) revealed a significant change in the elemental distribution. In the pristine particles, no considerable signals were observed for the elements Ba, Pb, and Zn, whereas significantly increased signals were found after the ageing experiment. This is consistent with a number of studies that have investigated the adsorption of metals on MPs in the natural environment, where a positive correlation was found between the adsorbed metals on MPs and the amount of biofilm (Liu et al., 2021). As in our study, Ba and Zn have predominantly been detected on aged MPs, but Sr, Pb, and Ca have also been found adsorbed on MPs sampled in the aquatic environment (Richard et al., 2019; Liu et al., 2021). However, the extent to which metals are adsorbed onto MPs depends on the physico-chemical properties of the particles (material, size, age, crystallinity, functional groups, and polarity), the composition and mass of the biofilm, and the physico-chemical properties of the surrounding environment (pH, ionic strength, and temperature) (Gao et al., 2021; Liu et al., 2022). In this context, different polymers showed significant differences in the adsorption capacity of the metals under different conditions. Moreover, the elements accumulated in the formed biofilm covering MPs play a crucial role in the overall toxicity of a particle (Kalčíková et al., 2020). In comparing the MPs aged in freshwater and wastewater, no obvious differences were observed between the two treatments. In both cases, Ba and Pb tended to accumulate on the MPs' surfaces, revealing the shapes of individual particles without diffusion into the bulk of the particles. In addition, Zn hotspots were detected and correlated with the Ba, Pb, and Ti hotspots.

For the PET, Sb present as an additive revealed the shapes and locations of individual particles (Fig. 5). Sb signals of the pristine and aged PET did not show a significant difference. This indicated that Sb did not leach significantly from the MPs during ageing. The pristine PET showed no significant signals of Ba, Pb, or Zn compared to the aged samples. Interestingly, looking at the Pb distribution, Pb was only found in the PET aged in freshwater in near-surface regions of the particles and the biofilm covering the particle. Other elements, such as Ba and Zn, were also found in the same regions as Pb. In wastewater-aged PET, Ba and Zn were also found in the near-surface regions of the particles.

Similar findings were achieved for the other polymer types, indicating the uptake of trace metals by various MPs during ageing in freshwater and wastewater. For example, the elemental maps presented for the PA (Fig. S15) show a homogeneous distribution of Ti and Ba in the MPs aged in freshwater and wastewater, which were not present in the pristine sample. This outcome indicated the diffusion and uptake of these elements into the bulk of the particles, whereas the uptake of Co and Pb occurred only on the particle surface. The pristine PVC and those aged in freshwater show a similar homogeneous distribution of Pb in the individual particles (Fig. S19), whereas Pb was not present in the PVC aged in wastewater. This indicates Pb contamination in the PVC samples during ageing in wastewater.

It should be noted that comparing qualitative LA-ICP-MS analysis with quantitative liquid ICP-MS analysis of digested particles is complicated, and various aspects must be considered. LA-ICP-MS data show the elemental distribution of a limited number of individual particles, whereas liquid ICP-MS analysis is the average result of 30 mg of sample, and thus, hundreds of particles. This difference in sampling size can naturally lead to deviations. In addition to the limited sampling size, LA-ICP-MS may offer better sensitivity for some elements than liquid ICP-MS analysis since the solid sample is analysed directly, and dilution steps necessary for liquid ICP-MS analysis can be avoided. For example, LA-ICP-MS analysis revealed Co in the pristine PVC particles, which was not detected with liquid ICP-MS (Fig. S19).

LA-ICP-MS offers significant insight into the fate of MPs when aged in freshwater and wastewater. Changes in the elemental composition within individual particles, as well as the adsorption and accumulation of inorganic constituents in a developed biofilm, can be investigated with this technique.

4. Conclusions

The reliable detection and monitoring of MPs is currently the greatest challenge for microplastic research and is critical for establishing monitoring campaigns worldwide. It is important to perform MP analysis with a minimum number of steps, as the possibility of loss, destruction, or contamination of samples is high. Moreover, the direct

detection of MPs, especially those largely covered with natural organic and inorganic matter or biofilm, remains a major challenge. However, the results of the present study show that when using advanced laser-based techniques, the identification and characterization of aged MPs covered by biofilms is possible. Therefore, these advanced techniques can largely complement conventional analytical methods and additionally provide new insights into the changes in the chemical composition and properties of aged particles. This preliminary study shows high feasibility, but future work needs to focus on the detection limits and interference with other (natural) particles. However, the promising results obtained here suggest that these techniques could not only be used for the detection of MPs in environmental samples but also (separately or in tandem) for the detection of MPs in biotic samples, especially for the accurate localization of MPs in tissues, which has not been possible so far. In addition to the importance of the development of analytical approaches to detect environmentally relevant MPs, the results of this study shed light on the ageing process of MPs and the change in MP properties, which are essential for understanding the fate of MPs in the aquatic environment.

Credit authors statement

Pavel Pořízka: Conceptualization, Methodology, Investigation, Writing – original draft, Visualization, Funding acquisition, Resources. Lukas Brunnbauer: Methodology, Investigation, Writing – original draft. Michaela Porkert: Methodology, Investigation. Ula Rozman: Investigation, Data curation, Methodology, Writing – original draft, Visualization. Gregor Marolt: Investigation. Daniel Holub: Investigation, Writing – original draft. Martin Kizovsky: Investigation, Writing – review & editing. Markéta Benešová; Investigation. Ota Samek: Investigation, Writing – review & editing, Funding acquisition. Andreas Limbeck: Methodology, Writing – original draft, Resources. Jozef Kaiser: Writing – original draft, Supervision, Funding acquisition. Gabriela Kalčíková; Conceptualization, Methodology, Investigation, Writing – original draft, Funding acquisition, Visualization, Resources, Supervision

Declaration of competing interest

The authors declare that they have no known competing financial interests or personal relationships that could have appeared to influence the work reported in this paper.

Data availability

Data will be made available on request.

Acknowledgement

The authors acknowledge the Chair of Wood Science and Technology, Biotechnical Faculty, University of Ljubljana, for lending a centrifugal mill, Mrs. Barbara Klun for the preparation of the microplastics, and Dr. Tina Skalar for the laboratory assistance in the characterization of the microplastics. PP gratefully acknowledges the support of the Czech Grant Agency (no. 20-19526Y); PP and JK acknowledge the support of the Czech Grant Agency (no. 22–04602L); JK and DH acknowledge the support of the Brno University of Technology (FSI–S-20-6353 and FV 22–11, respectively). This work was partially financed by the Slovenian Research Agency (research programs P2-0191, P1-0153, and the Plasti-C-Wetland project (J2-2491) (https://planterastics.fkkt.uni-lj.si/plasti-c-wetland). This article is based upon work from COST Action CA20101 Plastics monitoRIng detectiOn RemedIaTion recoverY - PRIORITY, supported by COST (European Cooperation in Science and Technology, www.cost.eu).

Appendix A. Supplementary data

Supplementary data to this article can be found online at https://doi.org/10.1016/j.chemosphere.2022.137373.

References

Anzano, J.M., Bello-Gálvez, C., Lasheras, R.J., 2014. Identification of polymers by means of LIBS. In: Musazzi, S., Perini, U. (Eds.), Laser-Induced Breakdown Spectroscopy: Theory and Applications. Springer Berlin Heidelberg, Berlin, Heidelberg, pp. 421–438.

Bonta, M., Gonzalez, J.J., Quarles, C.D., Russo, R.E., Hegedus, B., Limbeck, A., 2016. Elemental mapping of biological samples by the combined use of LIBS and LA-ICP-MS. J. Anal. At. Spectrom. 31, 252–258.

Brunnbauer, L., Mayr, M., Larisegger, S., Nelhiebel, M., Pagnin, L., Wiesinger, R., Schreiner, M., Limbeck, A., 2020. Combined LA-ICP-MS/LIBS: powerful analytical tools for the investigation of polymer alteration after treatment under corrosive conditions. Sci. Rep. 10, 12513.

Chamradová, I., Pořízka, P., Kaiser, J., 2021. Laser-Induced Breakdown Spectroscopy analysis of polymers in three different atmospheres. Polym. Test. 96, 107079.

Chen, D., Wang, T., Ma, Y., Wang, G., Kong, Q., Zhang, P., Li, R., 2020. Rapid characterization of heavy metals in single microplastics by laser induced breakdown spectroscopy. Sci. Total Environ. 743, 140850.

El Hadri, H., Gigault, J., Mounicou, S., Grassl, B., Reynaud, S., 2020. Trace element distribution in marine microplastics using laser ablation-ICP-MS. Mar. Pollut. Bull. 160, 111716.

Gajarska, Z., Brunnbauer, L., Lohninger, H., Limbeck, A., 2021. Identification of 20 polymer types by means of laser-induced breakdown spectroscopy (LIBS) and chemometrics. Anal. Bioanal. Chem. 413, 6581–6594.

Gao, X., Hassan, I., Peng, Y., Huo, S., Ling, L., 2021. Behaviors and influencing factors of the heavy metals adsorption onto microplastics: a review. J. Clean. Prod. 319, 128777.

Hahladakis, J.N., Velis, C.A., Weber, R., Iacovidou, E., Purnell, P., 2018. An overview of chemical additives present in plastics: migration, release, fate and environmental impact during their use, disposal and recycling. J. Hazard Mater. 344, 179–199.

He, S., Jia, M., Xiang, Y., Song, B., Xiong, W., Cao, J., Peng, H., Yang, Y., Wang, W., Yang, Z., Zeng, G., 2022. Biofilm on microplastics in aqueous environment: Physicochemical properties and environmental implications. J. Hazard Mater. 424, 127286.

Henkel, C., Hüffer, T., Hofmann, T., 2019. The leaching of phthalates from PVC can be determined with an infinite sink approach. MethodsX 6, 2729–2734.

Hermsen, E., Mintenig, S.M., Besseling, E., Koelmans, A.A., 2018. Quality criteria for the analysis of microplastic in biota samples: a critical review. Environ. Sci. Technol. 52, 10230–10240.

ISO 1183-1, 2019. Plastics — Methods for Determining the Density of Non-cellular Plastics — Part 1: Immersion Method, Liquid Pycnometer Method and Titration Method.

Jalón-Rojas, I., Romero-Ramírez, A., Fauquembergue, K., Rossignol, L., Cachot, J., Sous, D., Morin, B., 2022. Effects of biofilms and particle physical properties on the rising and settling velocities of microplastic fibers and sheets. Environ. Sci. Technol. 56, 8114–8123.

Jemec Kokalj, A., Kuehnel, D., Puntar, B., Žgajnar Gotvajn, A., Kalčikova, G., 2019. An exploratory ecotoxicity study of primary microplastics versus aged in natural waters and wastewaters. Environ. Pollut. 254, 112980.

Junjuri, R., Zhang, C., Barman, I., Gundawar, M.K., 2019. Identification of post-consumer plastics using laser-induced breakdown spectroscopy. Polym. Test. 76, 101–108.

Kalčíková, G., Skalar, T., Marolt, G., Jemec Kokalj, A., 2020. An environmental concentration of aged microplastics with adsorbed silver significantly affects aquatic organisms. Water Res. 175, 115644.

Kalčíková, G., Zupančič, M., Jemec, A., Žgajnar Gotvajn, A., 2016. The impact of humic acid on chromium phytoextraction by aquatic macrophyte Lemna minor. Chemosphere 147, 311–317.

Kameda, Y., Yamada, N., Fujita, E., 2021. Source- and polymer-specific size distributions of fine microplastics in surface water in an urban river. Environ. Pollut. 284, 117516.

Lagarde, F., Olivier, O., Zanella, M., Daniel, P., Hiard, S., Caruso, A., 2016. Microplastic interactions with freshwater microalgae: Hetero-aggregation and changes in plastic density appear strongly dependent on polymer type. Environ. Pollut. 215, 331–339.

Li, L., Li, M., Deng, H., Cai, L., Cai, H., Yan, B., Hu, J., Shi, H., 2018. A straightforward method for measuring the range of apparent density of microplastics. Sci. Total Environ. 639, 367–373.

Lichtenthaler, H.K., 1987. 34 Chlorophylls and carotenoids: Pigments of photosynthetic biomembranes. Methods Enzymol. 148, 350–382.

Liu, K., Tian, D., Li, C., Li, Y., Yang, G., Ding, Y., 2019. A review of laser-induced breakdown spectroscopy for plastic analysis. TrAC, Trends Anal. Chem. 110, 327–334.

Liu, S., Huang, J., Zhang, W., Shi, L., Yi, K., Yu, H., Zhang, C., Li, S., Li, J., 2022. Microplastics as a vehicle of heavy metals in aquatic environments: a review of adsorption factors, mechanisms, and biological effects. J. Environ. Manag. 302, 113995.

Liu, Z., Adyel, T.M., Miao, L., You, G., Liu, S., Hou, J., 2021. Biofilm influenced metal accumulation onto plastic debris in different freshwaters. Environ. Pollut. 285, 117646.

Long, M., Moriceau, B., Gallinari, M., Lambert, C., Huvet, A., Raffray, J., Soudant, P., 2015. Interactions between microplastics and phytoplankton aggregates: impact on their respective fates. Mar. Chem. 175, 39–46.
Lu, H.-C., Ziajahromi, S., Neale, P.A., Leusch, F.D.L., 2021. A systematic review of freshwater microplastics in water and sediments: Recommendations for harmonisation to enhance future study comparisons. Sci. Total Environ. 781, 146693.
Mariano, S., Tacconi, S., Fidaleo, M., Rossi, M., Dini, L., 2021. Micro and nanoplastics identification: classic methods and innovative detection techniques. Frontiers in Toxicology 3.
Marturano, V., Cerruti, P., Ambrogi, V., 2017. Polymer additives. Physical Sciences Reviews 2.
Menchaca, C., Alvarez-Castillo, A., Martinez-Barrera, G., Lopez-Valdivia, H., Carrasco, H., Castano, V.M., 2003. Mechanisms for the modification of nylon 6,12 by gamma irradiation. Int. J. Mater. Prod. Technol. 19, 521–529.
Meng, J., Xu, B., Liu, F., Li, W., Sy, N., Zhou, X., Yan, B., 2021. Effects of chemical and natural ageing on the release of potentially toxic metal additives in commercial PVC microplastics. Chemosphere 283, 131274.
Miao, L., Wang, C., Adyel, T.M., Wu, J., Liu, Z., You, G., Meng, M., Qu, H., Huang, L., Yu, Y., Hou, J., 2020. Microbial carbon metabolic functions of biofilms on plastic debris influenced by the substrate types and environmental factors. Environ. Int. 143, 106007.
Michel, A.P.M., Morrison, A.E., Preston, V.L., Marx, C.T., Colson, B.C., White, H.K., 2020. Rapid identification of marine plastic debris via spectroscopic techniques and machine learning classifiers. Environ. Sci. Technol. 54, 10630–10637.
Parrish, K., Fahrenfeld, N.L., 2019. Microplastic biofilm in fresh- and wastewater as a function of microparticle type and size class. Environ. Sci. J. Integr. Environ. Res.: Water Research & Technology 5, 495–505.
Pedregosa, F., Varoquaux, G., Gramfort, A., Michel, V., Thirion, B., Grisel, O., Blondel, M., Prettenhofer, P., Weiss, R., Dubourg, V., 2011. Scikit-learn: machine learning in Python. J. Mach. Learn. Res. 12, 2825–2830.
Pořízka, P., Klus, J., Képeš, E., Prochazka, D., Hahn, D.W., Kaiser, J., 2018. On the utilization of principal component analysis in laser-induced breakdown spectroscopy data analysis, a review. Spectrochim. Acta B Atom Spectrosc. 148, 65–82.
Prata, J.C., da Costa, J.P., Girão, A.V., Lopes, I., Duarte, A.C., Rocha-Santos, T., 2019. Identifying a quick and efficient method of removing organic matter without damaging microplastic samples. Sci. Total Environ. 686, 131–139.
Richard, H., Carpenter, E.J., Komada, T., Palmer, P.T., Rochman, C.M., 2019. Biofilm facilitates metal accumulation onto microplastics in estuarine waters. Sci. Total Environ. 683, 600–608.
Rozman, U., Kalčíková, G., 2022. Seeking for a perfect (non-spherical) microplastic particle – the most comprehensive review on microplastic laboratory research. J. Hazard Mater. 424, 127529.
Rozman, U., Turk, T., Skalar, T., Zupančič, M., Čelan Korošin, N., Marinšek, M., Olivero-Verbel, J., Kalčíková, G., 2021. An extensive characterization of various environmentally relevant microplastics – material properties, leaching and ecotoxicity testing. Sci. Total Environ. 773, 145576.
SAPEA, 2019. A Scientific Perspective on Microplastics in Nature and Society.
Shamskhany, A., Li, Z., Patel, P., Karimpour, S., 2021. Evidence of microplastic size impact on mobility and transport in the marine environment: a review and synthesis of recent research. Front. Mar. Sci. 8.
Shokri, A., Fard, M.S., 2022. A critical review in Fenton-like approach for the removal of pollutants in the aqueous environment. Environmental Challenges 7, 100534.
Sommer, C., Schneider, L.M., Nguyen, J., Prume, J.A., Lautze, K., Koch, M., 2021. Identifying microplastic litter with laser induced breakdown spectroscopy: a first approach. Mar. Pollut. Bull. 171, 112789.
Song, Y.K., Hong, S.H., Jang, M., Han, G.M., Rani, M., Lee, J., Shim, W.J., 2015. A comparison of microscopic and spectroscopic identification methods for analysis of microplastics in environmental samples. Mar. Pollut. Bull. 93, 202–209.
Stehrer, T., Heitz, J., Pedarnig, J.D., Huber, N., Aeschlimann, B., Günther, D., Scherndl, H., Linsmeyer, T., Wolfmeir, H., Arenholz, E., 2010. LA-ICP-MS analysis of waste polymer materials. Anal. Bioanal. Chem. 398, 415–424.
Strasser, R.J., Govindjee, 1992. The fo and the O-J-I-P fluorescence rise in higher plants and algae. In: Argyroudi-Akoyunoglou, J.H. (Ed.), Regulation of Chloroplast Biogenesis. Springer US, Boston, MA, pp. 423–426.
Tu, C., Liu, Y., Li, L., Li, Y., Vogts, A., Luo, Y., Waniek, J.J., 2021. Structural and functional characteristics of microplastic associated biofilms in response to temporal dynamics and polymer types. Bull. Environ. Contam. Toxicol. 107, 633–639.
Venable, M.E., Podbielski, M.R., 2019. Impact of substrate material on algal biofilm biomass growth. Environ. Sci. Pollut. Control Ser. 26, 7256–7262.
Vikhareva, I.N., Aminova, G.K., Moguchev, A.I., Mazitova, A.K., 2021. The effect of a zinc-containing additive on the properties of PVC compounds. Adv. Polym. Technol. 2021, 5593184.
Wang, Q., Wangjin, X., Zhang, Y., Wang, N., Wang, Y., Meng, G., Chen, Y., 2020. The toxicity of virgin and UV-aged PVC microplastics on the growth of freshwater algae Chlamydomonas reinhardtii. Sci. Total Environ. 749, 141603.
Welle, F., Franz, R., 2011. Migration of antimony from PET bottles into beverages: determination of the activation energy of diffusion and migration modelling compared with literature data. Food Addit. Contam. 28, 115–126.
Xia, B., Sui, Q., Du, Y., Wang, L., Jing, J., Zhu, L., Zhao, X., Sun, X., Booth, A.M., Chen, B., Qu, K., Xing, B., 2022. Secondary PVC microplastics are more toxic than primary PVC microplastics to Oryzias melastigma embryos. J. Hazard Mater. 424, 127421.
Xu, J.-L., Thomas, K.V., Luo, Z., Gowen, A.A., 2019. FTIR and Raman imaging for microplastics analysis: state of the art, challenges and prospects. TrAC, Trends Anal. Chem. 119, 115629.